

# PPAR $\gamma$ coactivator-1 $\alpha$ contributes to exercise-induced regulation of intramuscular lipid droplet programming in mice and humans

Timothy R. Koves,<sup>1,\*†</sup> Lauren M. Sparks,<sup>1,§,\*\*\*</sup> J. P. Kovalik,<sup>\*</sup> Merrie Mosedale,<sup>\*</sup> Ramamani Arumugam,<sup>\*</sup> Karen L. DeBalsi,<sup>\*</sup> Karen Everingham,<sup>†††</sup> Leigh Thorne,<sup>§§</sup> Esther Phielix,<sup>§</sup> Ruth C. Meex,<sup>\*\*\*</sup> C. Lawrence Kien,<sup>†††</sup> Matthijs K. C. Hesselink,<sup>\*\*\*</sup> Patrick Schrauwen,<sup>1,2,§</sup> and Deborah M. Muoio<sup>1,2,\*†,§§§</sup>

Sarah W. Stedman Nutrition & Metabolism Center,<sup>\*</sup> Department of Medicine,<sup>†</sup> and Department of Pharmacology & Cancer Biology,<sup>§§§</sup> Duke University, Durham, NC; Department of Human Biology<sup>§</sup> and Department of Human Movement Sciences,<sup>\*\*\*</sup> Nutrition and Toxicology Research Institute Maastricht (NUTRIM), Maastricht University, Maastricht, The Netherlands; Translational Research Institute for Metabolism and Diabetes,<sup>\*\*</sup> Florida Hospital, Orlando, FL; Department of Medicine<sup>††</sup> and Department of Pediatrics and Medicine,<sup>†††</sup> University of Vermont, Colchester, VT; and Department of Pathology & Laboratory Medicine,<sup>§§</sup> University of North Carolina, Chapel-Hill, NC

**Abstract** Intramuscular accumulation of triacylglycerol, in the form of lipid droplets (LD), has gained widespread attention as a hallmark of metabolic disease and insulin resistance. Paradoxically, LDs also amass in muscles of highly trained endurance athletes who are exquisitely insulin sensitive. Understanding the molecular mechanisms that mediate the expansion and appropriate metabolic control of LDs in the context of habitual physical activity could lead to new therapeutic opportunities. Herein, we show that acute exercise elicits robust upregulation of a broad program of genes involved in regulating LD assembly, morphology, localization, and mobilization. Prominent among these was perilipin-5, a scaffolding protein that affects the spatial and metabolic interactions between LD and their surrounding mitochondrial reticulum. Studies in transgenic mice and primary human skeletal myocytes established a key role for the exercise-responsive transcriptional coactivator PGC-1 $\alpha$  in coordinating intramuscular LD programming with mitochondrial remodeling. Moreover, translational studies comparing physically active versus inactive humans identified a remarkably strong association between expression of intramuscular LD genes and enhanced insulin action in exercise-trained subjects. These results reveal an intimate molecular connection between intramuscular LD biology and mitochondrial metabolism that could prove relevant to the etiology and treatment of insulin resistance and other disorders of lipid imbalance.—Koves, T. R., L. M. Sparks,

J. P. Kovalik, M. Mosedale, R. Arumugam, K. L. DeBalsi, K. Everingham, L. Thorne, E. Phielix, R. C. Meex, C. L. Kien, M. K. C. Hesselink, P. Schrauwen, and D. M. Muoio. **PPAR $\gamma$  coactivator-1 $\alpha$  contributes to exercise-induced regulation of intramuscular lipid droplet programming in mice and humans.** *J. Lipid Res.* 2013. 54: 522–534.

**Supplementary key words** skeletal muscle • athlete's paradox • mitochondria • fatty acid metabolism • insulin sensitivity • gene regulation

Although white adipocytes are best known as the cell type that sequesters large quantities of neutral lipid, most eukaryotic cells, including skeletal myocytes, form lipid droplets. Current interests in intramyocellular triacylglycerol (IMTG) stem largely from their infamous association with metabolic disease (reviewed in Refs. 1, 2). Thus, in the context of obesity and type 2 diabetes, IMTG content

Abbreviations: ATGL, adipose triglyceride lipase; BMI, body mass index; DAG, diacylglycerol; EDL, extensor digitorum longus; EE, energy expenditure; G0S2, G0/G1 switch 2; HF, high fat; HSkMC, human skeletal myotube; IMCL, intramyocellular lipid; IMTG, intramyocellular triacylglycerol; NT, nontransgenic; LD, lipid droplet; PGC-1 $\alpha$ , PPAR $\gamma$  coactivator-1 $\alpha$ ; PLIN5, perilipin family protein 5; PPAR, peroxisome proliferator-activated receptor; Rd, whole-body glucose disposal;  $\Delta$ Rd, change in whole-body glucose disposal (insulin sensitivity); RQ, respiratory quotient;  $\Delta$ RQ, change in respiratory quotient (metabolic flexibility); SC, standard chow; SCD1, stearoyl-CoA desaturase 1; TA, tibialis anterior; TAG, triacylglycerol; VO<sub>2</sub> max, maximal oxygen consumption per kilogram of body weight as measured during maximal exercise test; Wmax, maximum watts achieved per kilogram of body weight as measured during a maximal exercise test.

<sup>1</sup>T. R. Koves, L. M. Sparks, P. Schrauwen, and D. M. Muoio contributed equally to this work.

<sup>2</sup>To whom correspondence should be addressed.  
e-mail: muoio@duke.edu (D.M.M.); p.schrauwen@maastrichtuniversity.nl (P.S.)

This work was supported by National Institutes of Health Grants R01-AG-028930 (D.M.) and R01-DK-073284 (L.K. and D.M.); the American Diabetes Association (D.M.); Ellison Medical Foundation Grant AG-NS-0548-09 (T.K.); Dutch Diabetes Research Foundation Grant 2004.00.059; and VICI Grants 918.96.618 (P.S.) and 917.66.359 (M.H.) for innovative research from the Netherlands Organization for Scientific Research (NWO). The contents of this work are solely the responsibility of the authors and do not necessarily represent the official views of the National Institutes of Health.

Manuscript received 29 May 2012 and in revised form 27 October 2012

Published, JLR Papers in Press, November 21, 2012  
DOI 10.1194/jlr.P028910

correlates inversely with muscle insulin sensitivity and serves as a strong predictor of diabetes risk (3–5). It is noteworthy, however, that intramuscular lipid accumulation is not strictly a pathologic phenomenon. For example, lipid content is elevated in red compared with white skeletal muscles and increases in response to habitual exercise in both oxidative and glycolytic fibers (6). Paradoxically, endurance-trained athletes have elevated IMTG content, in some cases exceeding that measured in type 2 diabetic subjects (3, 6), but they retain exquisite insulin sensitivity.

Despite decades of intense interest in skeletal muscle lipid metabolism, the precise molecular mechanisms that link oxidative fiber type and contractile activity to increased IMTG content and enhanced control of lipid droplet metabolism have remained relatively understudied. Given the intimate spatial and functional relationship between muscle lipid droplets and the surrounding mitochondrial reticulum (shown herein and elsewhere) (7), we hypothesized that myocellular genesis of these two interconnected organelles might be regulated by a common molecular switch. We show here that exercise-induced activation of the mitochondrial program in skeletal muscle is indeed paralleled by transcriptional induction of a large set of genes that controls lipid droplet assembly as well as fatty acid flux in and out of the IMTG pool. A similar set of lipid droplet genes is likewise regulated by PPAR $\gamma$  coactivator-1 $\alpha$  (PGC-1 $\alpha$ ), an exercise-responsive transcriptional coactivator known to play a major role in adaptive remodeling of muscle mitochondria. In aggregate, results of this study establish a novel role for PGC-1 $\alpha$  in regulating skeletal muscle storage and turnover of IMTG, which in turn appears to impact mitochondrial fuel selection at multiple levels.

## RESEARCH DESIGN AND METHODS

### Animals

Studies were conducted in accordance with Duke University Institutional Animal Care and Use Committee using male and female C57/Bl6J mice or MCK-PGC-1 $\alpha$  transgenic mice (kindly provided by Dr. Bruce Spiegelman, Harvard University) and littermate controls. Mice were housed in a temperature-controlled environment with a 12:12 h light/dark cycle and provided ad libitum access to Purina standard chow (SC) or high-fat diet (HF; Research Diets 45% fat) and water.

### Transmission electron microscopy

Tibialis anterior (TA) muscles from female C57/Bl6J mice on either SC or HF diets and MCK-PGC-1 $\alpha$  transgenic mice were removed in the fed state after Nembutal, immersed in 2% formaldehyde/2.5% glutaraldehyde, and processed using standard methods (8) at the Translational Core Facility at UNC-Chapel Hill.

### Muscle incubations

Fatty acid oxidation and incorporation into glycerol lipids in mouse soleus and extensor digitorum longus (EDL) muscles was assessed as described (9). A similar buffer containing 5.5 mM glucose (2  $\mu$ Ci per ml [ $U$ - $^{14}$ C]glucose) was used for measurement of

glucose oxidation in muscles preincubated 30 min in  $\pm$ 100  $\mu$ M sodium etomoxir (Sigma-Aldrich).

### Acute exercise, gene expression, and Western blotting (mouse)

Twelve-week-old male C57/Bl6J mice ( $n = 4$ ) were habituated to the treadmill (3M/6M Columbus Instruments) for three days. Exercise began at 0900 h after food withdrawal at 0800 h. After a warm-up at 5 m/min, speed was increased to 10 m/min for 20 min, and then 1 m/min to a final rate of 15 m/min, which was maintained for 1 h. Running was encouraged by gentle shock. Mice were anesthetized (100 mg/kg Nembutal) immediately postexercise or after 3 or 24 h of recovery. Control and MCK-PGC-1 $\alpha$  transgenic mice were habituated but not exercised. TA muscles were excised and flash frozen. RT-PCR was performed using specific TaqMan assays (Applied Biosystems) on a Prism 7000. Western blot analysis (10) used the following antibodies: anti-PGC-1 $\alpha$  (Chemicon or Calbiochem), anti-MLDP (Plin5/OxPAT; American Research Products), or anti-ADRP (Plin2; Fitzgerald). Blots were normalized to total protein determined by Memcode Reversible Protein Stain (Thermo-Fisher Scientific).

### Lipid analyses

Analysis of glycerolipid lipid synthesis in cultured cells and mouse muscle were as previously described (9, 11). Quantitative analysis of total lipids and fatty acid composition in mouse TA muscles was performed using 10–20 mg of flash-frozen powdered tissue diluted 20-fold and homogenized in methanol. Diacylglycerols (DAG) and triacylglycerols (TAG) were extracted in methanol-chloroform and separated by thin-layer chromatography before analysis of the esterified fatty acids by GC/MS (12).

### Human skeletal muscle cells

Human skeletal myocytes were isolated, expanded, and differentiated as detailed in Ref. 11. On differentiation day 4, cells were treated for 24 h with viruses encoding either  $\beta$ -galactosidase or PGC-1 $\alpha$  virus. Experimental treatments are described in the figure legends. During the pulse-chase experiments, 250  $\mu$ l of medium was transferred to septum-sealed tubes and acidified for assessment of oxidation products ( $^{14}$ CO $_2$  and  $^{14}$ C-ASM) (11). Total RNA was isolated using Qiagen RNeasy kits and gene expression was evaluated using TaqMan RT-PCR. Fluorometric analysis of neutral lipid was performed on myotubes incubated with AdipoRed as per the manufacturer's instructions (Cambrex). Recombinant adenoviruses encoding mouse PGC-1 $\alpha$  and mouse perilipin 1 were kind gifts from Drs. Bruce Spiegelman and Andrew Greenberg, respectively. Adenoviruses were amplified and purified using published methods (13).

### Human studies

Procedures were approved by the Institutional Medical Ethical Committee of Maastricht University. After providing informed written consent, a cohort of 19 lean, young endurance-trained ( $n = 9$ ) and untrained ( $n = 10$ ) male volunteers underwent physical examination and physiological assessment. Body composition and insulin sensitivity were evaluated by hydrostatic weighing and a 6 h euglycemic-hyperinsulinemic clamp, respectively. Trained subjects participated in endurance exercises three times a week for at least two consecutive years prior to study participation and had a VO $_2$  max above 55 ml kg $^{-1}$  min $^{-1}$ . Untrained subjects had a sedentary lifestyle and a VO $_2$  max below 45 ml kg $^{-1}$  min $^{-1}$ . Subjects were asked to refrain from exercise the last 48 h prior to the testing, and dietary intake was maintained during the last three days before each clamp with a standardized meal provided on the last day. Power calculations to determine subject numbers were

calculated based on the change in insulin sensitivity as measured by the euglycemic-hyperinsulinemic clamp.

### Euglycemic-hyperinsulinemic clamp

A constant infusion of glucose tracer ([6,6- $^2\text{H}_2$ ] glucose) was initiated at  $t = -60$  min to determine insulin-stimulated glucose disposal in overnight-fasted subjects. At  $t = 0$ , the actual clamp procedure was started with a constant coinfusion of insulin ( $40 \text{ mU m}^{-2} \text{ min}^{-1}$ ) and glycerol combined with the infusion of a variable amount of a 20% glucose solution to maintain euglycemia at  $5 \text{ mmol/L}$ . In the basal period ( $t = -30$  to  $0$ ) and under steady-state clamp conditions ( $t = 330$ – $360$ ), blood was sampled and indirect calorimetry (ventilated hood) was performed. Biopsies from the vastus lateralis were obtained under local anesthesia (2% lidocaine) using the Bergstrom technique before and after the clamp. Subjects were instructed to keep a constant eating pattern and refrain from physical activity 48 h prior to the clamp. Nonoxidative glucose disposal (NOGD) was calculated as Rd minus carbohydrate oxidation. Metabolic flexibility ( $\Delta\text{RQ}$ ) was expressed as the change in respiratory quotient from the fasted state to the insulin-stimulated condition.

### Human muscle biochemistry

Fresh cryosections ( $5 \mu\text{m}$ ) of skeletal muscle tissue were stained for intramyocellular lipid (IMCL) content by Oil Red O staining combined with fiber-typing and immunolabeling of the basal membrane marker laminin to allow quantification of IMCL as previously described (14). Total RNA was isolated from  $\sim 20 \text{ mg}$  of skeletal muscle tissue using acid phenol extraction and ethanol precipitation (15). Primers and probes were designed using Primer Express version 2.1 (Applied Biosystems), and sequences can be provided upon request. Real-time qRT-PCR (16) was performed as one-step reactions in Prism 7900 (Applied Biosystems) with GAPDH used as internal control. Tissues homogenates were prepared in RIPA-buffer [1% NP40, 0.5% SDS, 1 mM PMSF, 1 mM EDTA, Complete Inhibitor (Roche Diagnostics) in PBS, pH 7.4], and the  $15,000 \text{ g}$  supernatants were stored at  $-80^\circ\text{C}$  before Western blot analysis using the following antibodies: ATGL (Cell Signaling Technology), CGI-58 (Novus Biologicals), PLIN2 (Progen Biotechnik), and PLIN5 (Progen Biotechnik). Protein contents were determined by immunoblotting with near-infrared detection (Odyssey, Licor). To adjust for intergel variation, the optical density of the band of interest per subject was normalized to the mean optical density of the complete gel.

### Statistics

Statistical analyses were performed using JMP version 8.0 (SAS). Differences between groups were detected by unpaired  $t$ -tests. A two-way ANOVA model for repeated measures was applied using trained and untrained as between-subject variables and basal and insulin-stimulated data as repeated within-subject variables. Gene expression and clinical data were correlated using linear regression analysis. To investigate the influence of training on insulin sensitivity and metabolic flexibility, stepwise linear regression analyses for trained and untrained subjects were performed separately. Type I error rate was set a priori at  $P < 0.05$ .

## RESULTS

Shown by transmission electron microscopy, lipid droplets are larger and more numerous in red compared with white regions of mouse quadriceps, and in both fiber types the droplets are bordered by intermyofibrillar mitochondria

(Fig. 1A, B). This microstructural organization was maintained and even exaggerated in mouse TA muscles after several weeks of high-fat feeding (Fig. 1C, D). These images underscore the potential of muscle lipid droplets to modulate mitochondrial access to fatty acid fuel and to provide substrate during exercise (17). To assess the dynamic nature of IMTG in the absence of contractile activity and/or other lipolytic stimuli, we performed a pulse-chase experiment by exposing isolated mouse soleus and EDL muscles to [ $^{14}\text{C}$ ]oleate for 1 h, followed by a second hour of incubation without radioactive substrate. Predictably, rates of fatty acid incorporation into triacylglycerol was  $\sim 3$ -fold greater in soleus than in EDL. During the chase period, [ $^{14}\text{C}$ -oleate]labeling of the IMTG pool decreased 43% and 52% in soleus and EDL, respectively, indicating a high turnover rate under these conditions (Fig. 1E). Recovery of  $^{14}\text{CO}_2$ , reflecting oxidation of IMTG-derived fatty acids, was 1.75-fold greater in soleus compared with EDL, thus matching the relative abundance of TAG in these tissues (Fig. 1F). A second experiment sought to evaluate use of naturally deposited IMTG. To this end, we measured oxidation of [UL- $^{14}\text{C}$ ]glucose in isolated muscles treated with 0 or  $100 \mu\text{M}$  etomoxir, a potent inhibitor of carnitine palmitoyltransferase 1 and long-chain fatty acid oxidation (Fig. 1G). Exogenously supplied fatty acids were omitted from the incubation buffer; thus, effects of the inhibitor were attributed to metabolism of endogenous lipid. Addition of etomoxir increased rates of glucose oxidation 40% and 70% in soleus and EDL, respectively, implying that IMTG-derived fatty acids compete with glucose for use as an oxidative substrate (18), even in quiescent muscles from lean animals on a low-fat diet.

The physical and functional interplay between muscle lipid droplets and their neighboring mitochondria (Fig. 1A–D) suggested that assembly and activity of these two organelles might be regulated in a coordinated fashion. To test whether such regulation occurs at a genomic level, mice were subjected to an acute bout of treadmill exercise, a well-characterized physiological stimulus of both PGC-1 $\alpha$  and mitochondrial biogenesis (19–22). PGC-1 $\alpha$  mRNA increased transiently in response to contractile activity, peaking at 3 h postexercise and nearly returning to baseline levels within 24 h of recovery (Fig. 2A). RT-PCR analyses revealed a similar pattern for multiple genes involved in triacylglycerol synthesis as well as lipid droplet assembly, morphology, and mobilization (Fig. 2A), including diacylglycerol acyltransferase 1 (Dgat1), Lipin 1 (Lpin1), stearoyl-CoA desaturase (Scd1), the fat storage-inducing transmembrane proteins 1 and 2 (Fitm1/Fitm2), fat-specific protein 27 (Fsp27), perilipins 2–5 (Plin2–5), hormone-sensitive lipase (Hsl), adipose triglyceride lipase (Atgl/Pnpla2), Cgi-58, and G0/G1 switch gene 2 (G0s2) (23). Glycerol kinase and B2M (used as an endogenous control) were unaffected by acute exercise (Fig. 2A). Also upregulated by the exercise regimen were several nuclear receptors that are known partners of PGC-1 $\alpha$ ; these included LXR $\alpha$ , ERR $\alpha$ , and PPAR $\alpha$  (Fig. 2B).

We next evaluated TA muscles from MCK-PGC-1 $\alpha$  transgenic mice, which overexpress PGC-1 $\alpha$  specifically in



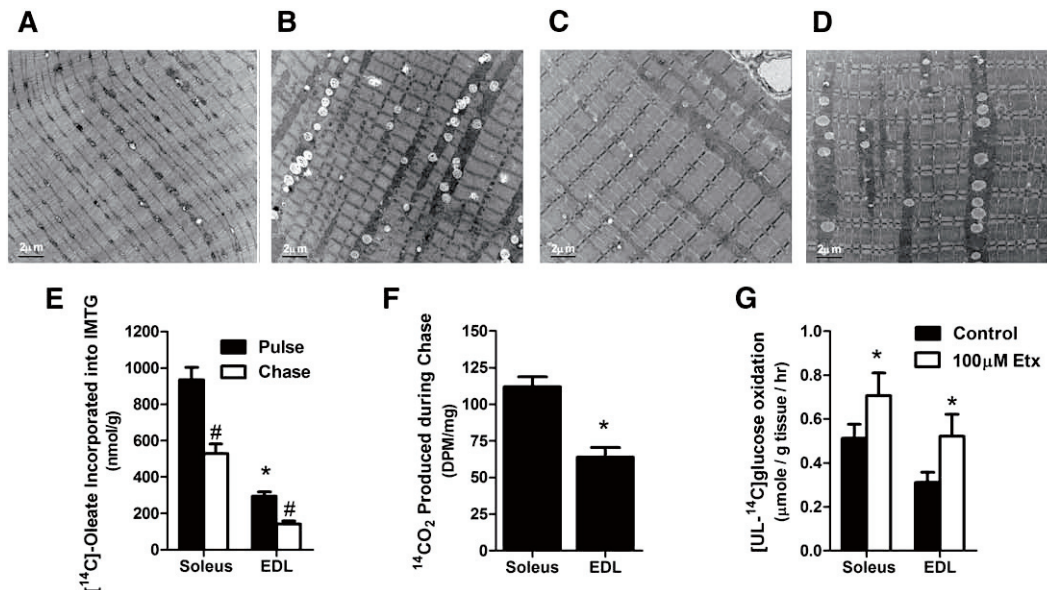


**Fig. 1.** Intramuscular lipid droplets are physically and functionally associated with skeletal muscle mitochondria. (A–D) Electron micrographs showing presence of mitochondria and lipid droplets in white (A) versus red (B) quadriceps muscle and in the tibialis anterior muscle of standard chow (C) versus high-fat (D) diet fed animals (bar = 2  $\mu$ m). (E) Accumulation and depletion of [ $^{14}$ C]labeled triacylglycerol in mouse soleus and extensor digitorum longus (EDL) muscles pulsed for 1 h with 1 mM [ $^{14}$ C]oleic acid in KHB buffer supplemented with 1% BSA and 0.5 mM L-carnitine followed by a 1 h chase in the absence of exogenous fatty acid. (F) Glycerolipid-derived  $^{14}$ CO $_2$  produced during the 1 h chase. (G) Oxidation of 5 mM [U- $^{14}$ C]glucose by isolated mouse muscle during a 1 h incubation in KHB buffer  $\pm$  100  $\mu$ M etomoxir (Etx). Values are means  $\pm$  SE (n = 5–6 muscles per group). \* $P$  < 0.05 versus soleus muscle; # $P$  < 0.05 versus pulse or control condition.

muscle (24). Similar to the exercise response, the MCK-PGC-1 $\alpha$  mice had 5-fold higher mRNA levels of PGC-1 $\alpha$  as well as a large subset of the lipid droplet genes compared with their nontransgenic (NT) counterparts (Fig. 2C). Interestingly, Plin5/OxPAT, which belongs to a family of lipid coat proteins (25), was the only perilipin member for which mRNA levels were upregulated in the MCK-PGC-1 $\alpha$  mice. Western blot analyses confirmed robust inductions of Plin5/OxPAT and ATGL protein expression in the transgenic mice (5.7- and 3-fold, respectively; Fig. 2D). Despite no change in mRNA levels of Plin2/Adrp, abundance of this lipid droplet protein was increased 3.3-fold in the transgenic muscles, suggesting posttranscriptional regulation as previously described (26). Electron microscopy revealed a PGC-1 $\alpha$ -associated increase in lipid droplet size and number (Fig. 3A), which was subsequently confirmed by quantitative biochemical analysis of the contralateral TA muscles. PGC-1 $\alpha$  overexpression increased total TAG and DAG content by 2.4- and 2.2-fold respectively (Fig. 3B), and it shifted the fatty acid composition of these glycerolipids toward an enrichment of the unsaturated 18:1 and 18:2 species (Fig. 3C–F). In aggregate, these data show that acute exercise activates the lipid droplet program, and they support a role for PGC-1 $\alpha$  in mediating this response.

To determine whether PGC-1 $\alpha$ -induced regulation of muscle lipid droplet metabolism occurs in a cell-autonomous manner independent of developmental and/or environmental factors, we used recombinant adenovirus to

overexpress mouse PGC-1 $\alpha$  in primary human skeletal myotubes (HskMC). rAd-mPGC-1 $\alpha$  elicited a dose-dependent increase in protein abundance compared with low expression levels in HskMC treated with the rAd- $\beta$ -gal control virus (Fig. 4A). For subsequent experiments, a viral dose of  $2.6 \times 10^8$  PFU/cm $^2$  was used to mimic the modest increase in muscle PGC-1 $\alpha$  protein content achieved by exercise training (10, 27). In addition to a classic panel of mitochondrial oxidative genes (10, 27), rAd-mPGC-1 $\alpha$  activated several mRNAs encoding proteins involved in lipid droplet assembly and metabolism (Fig. 4B). Likewise, staining with AdipoRed, a neutral lipid adherent fluorometric dye, revealed higher lipid content in rAd-mPGC-1 $\alpha$ -treated cells (Fig. 4C).

The impact of PGC-1 $\alpha$  on myocyte lipid synthesis and turnover was evaluated using the pulse-chase protocol illustrated in Fig. 4D. HskMC pretreated with  $\beta$ -gal or PGC-1 $\alpha$  adenovirus were exposed to [ $^{14}$ C]oleic acid for 24 h. During the pulse phase of the experiment, L-carnitine was omitted from the culture medium to disallow fat oxidation and limit confounding effects of enhanced oxidative capacity in the rAd-mPGC-1 $\alpha$  group. Carnitine was added to chase medium to permit normal use of lipid substrate during this period. Analysis of cellular glycerolipids by TLC and autoradiography revealed a clear PGC-1 $\alpha$  effect on labeling and turnover of TAG (Fig. 4E, F). During the 24 h pulse, [ $^{14}$ C]oleate incorporation into TAG was 1.5-fold greater in HskMC treated with rAd-mPGC-1 $\alpha$  compared with the control condition (Fig. 4F); whereas labeling of

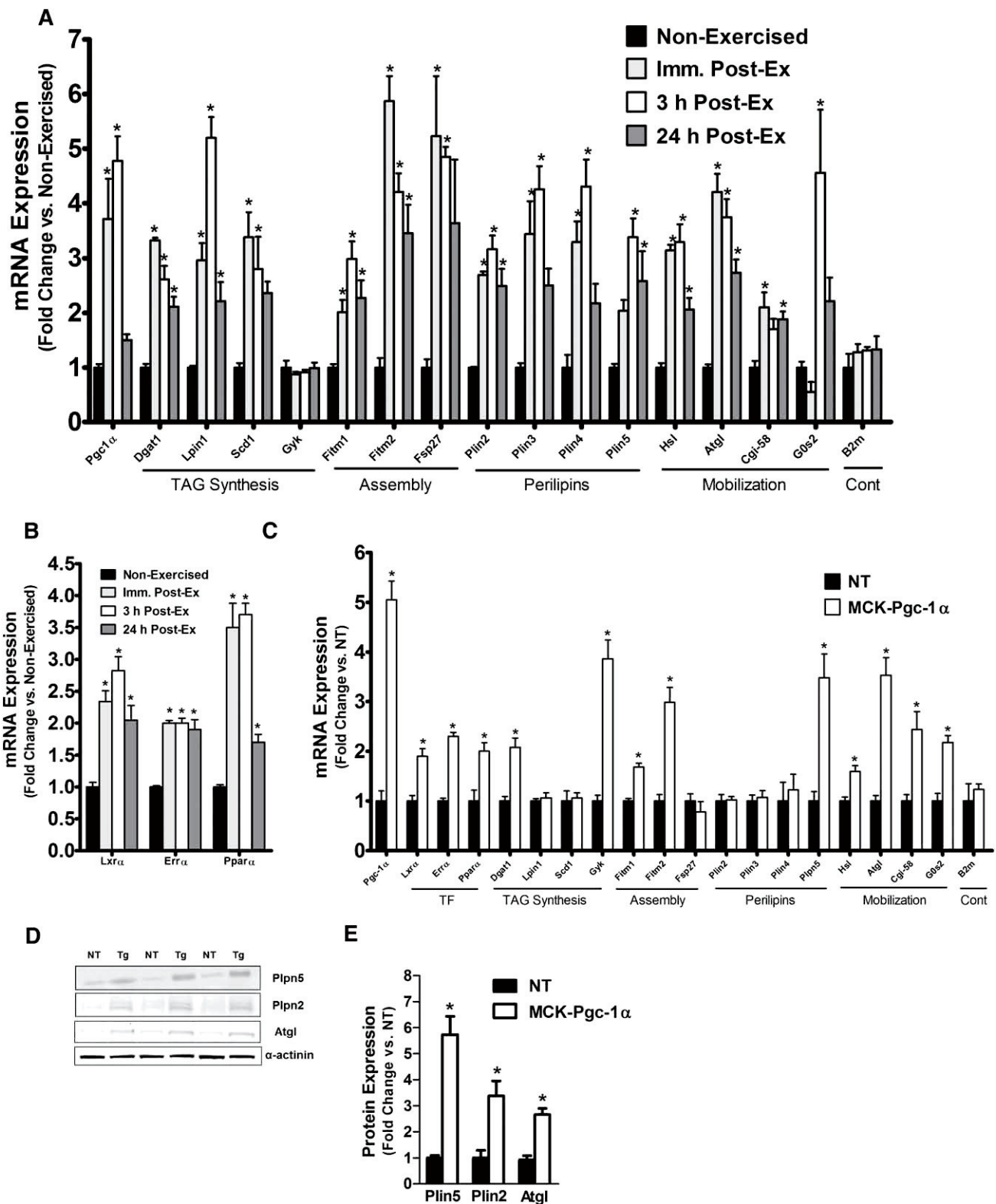


**Fig. 2.** Acute exercise and Pgc-1 $\alpha$  overexpression stimulate transcriptional induction of the lipid droplet program in mouse skeletal muscle. Expression of genes involved in lipid droplet metabolism were measured in the TA muscles of (A) wild-type mice at rest and following 90 min of treadmill exercise and (B–E) MCK-Pgc-1 $\alpha$  mice and NT littermates. Wild-type mice were euthanized at the indicated time points after exercise. TA muscles from NT or MCK-Pgc-1 $\alpha$  transgenic mice were used for gene expression and protein content. (B and C) Gene expression data for key transcription factors and lipid droplet metabolism. (D and E) Representative Western blot and protein quantification of Plin5 (perilipin 5/OxPAT), Plin2 (perilipin 2/Adrp), and ATGL (adipose tissue triglyceride lipase) protein abundance. Data represent means  $\pm$  SE for  $n = 4$  mice per group. \* $P < 0.05$  versus nonexercised or NT controls.

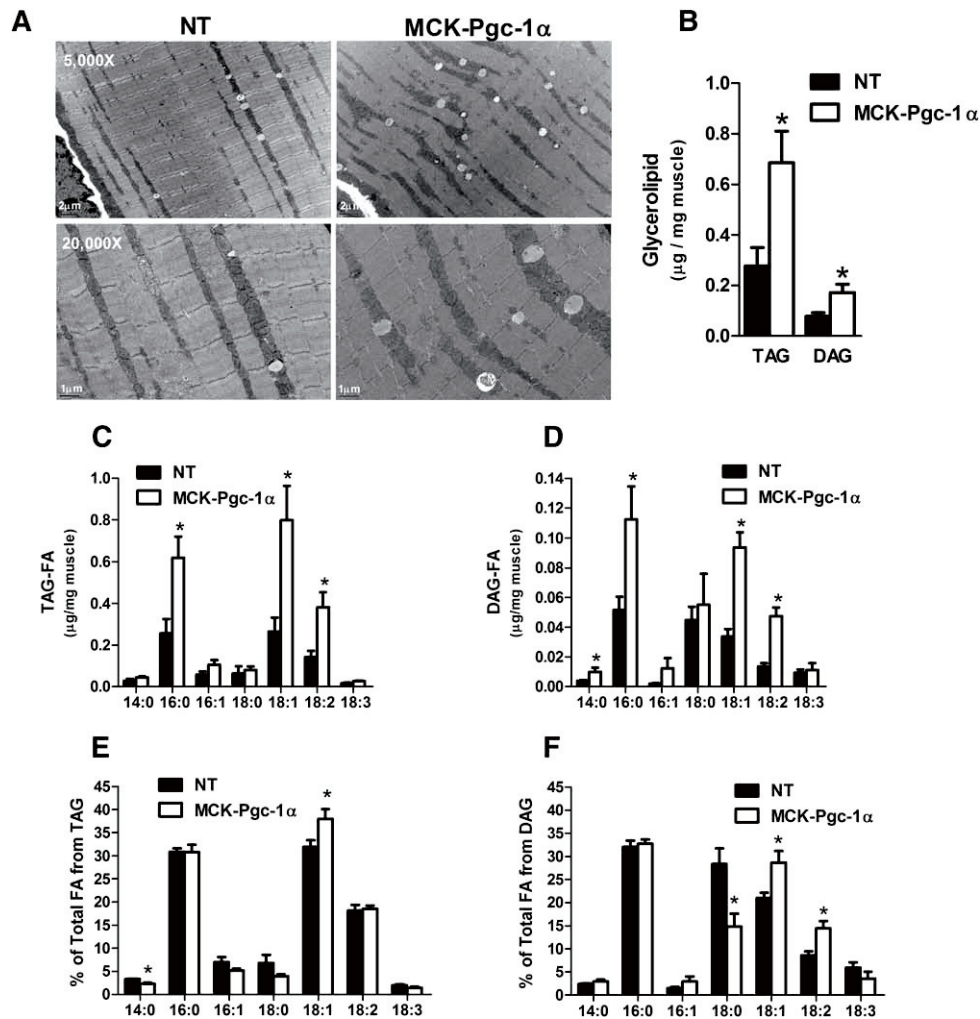


**Fig. 3.** Pgc-1 $\alpha$  overexpression promotes desaturation of muscle lipids. (A) Electron microscopy (bar = 1 or 2  $\mu$ m as noted) and (B) measurement of intramuscular TAG and DAG. Fatty acid composition of (C) TAG and (D) DAG in TA muscles from MCK-Pgc-1 $\alpha$  mice and NT littermates. (E and F) Fatty acid composition of muscle glycerolipids expressed as percentages of the total fatty acids present in either TAG or DAG. Data are means  $\pm$  SE for  $n = 4$  animals per group. \* $P < 0.05$  versus NT controls.

DAG and phospholipid pools was either unchanged or only minimally affected (Fig. 4G, H). PGC-1 $\alpha$  overexpression augmented loss of label from the TAG pool during the chase period, which corresponded with enhanced oxidation of endogenously-derived [ $1\text{-}^{14}\text{C}$ ]fatty acid (Fig. 4I). Interestingly, glycerol release was lower in the rAd-mPGC-1 $\alpha$  group at time 0 (pulse phase) and at 24 h, suggesting decreased lipolysis at those time points (Fig. 4J). We therefore surmised that under basal conditions (absence of lipolytic stimuli), PGC-1 $\alpha$  overexpression might encourage myocyte reesterification of glycerol and/or partially hydrolyzed TAG. Fitting with this presumption, rAd-mPGC-1 $\alpha$  increased HSkMC mRNA expression of DGAT1 and glycerol kinase, both of which promote reesterification and were likewise upregulated in MCK-PGC-1 $\alpha$  transgenic mice (Fig. 2B).

Emerging evidence suggests that IMTG-derived fatty acids regulate muscle expression of nuclear-encoded mitochondrial genes (28–30). To further explore this possibility in HSkMC, we used both genetic and pharmacological

strategies to perturb fatty acid trafficking through the lipid droplet. Our initial approach exploited the first-identified member of the PAT-family, perilipin 1 (Plin1), an adipocyte-specific protein that promotes lipid droplet formation and antagonizes TAG hydrolysis in the absence of lipolytic stimuli (31, 32). As expected, ectopic overexpression of Plin1 in HSkMC resulted in the sequestering of fatty acids in the lipid droplet compartment, evidenced by increased AdipoRed staining (Fig. 5A) and diminished glycerol release (Fig. 5B). Plin1-mediated disruption of lipid droplet turnover dampened HSkMC transcript levels of several classic targets of the peroxisome proliferator-activated receptor (PPAR) family of nuclear receptors, despite ample provision of PPAR-activating fatty acids (Fig. 5C). Likewise, treatment of HSkMC with the pharmacological lipase inhibitor diethylumbelliferyl phosphate (DEUP) (33) decreased mRNA expression of the same panel of PPAR-targeted genes (Fig. 5D). Thus, PGC-1 $\alpha$ -mediated regulation of lipid droplet metabolism might contribute to adaptive remodeling of muscle mitochondria (Fig. 5E).



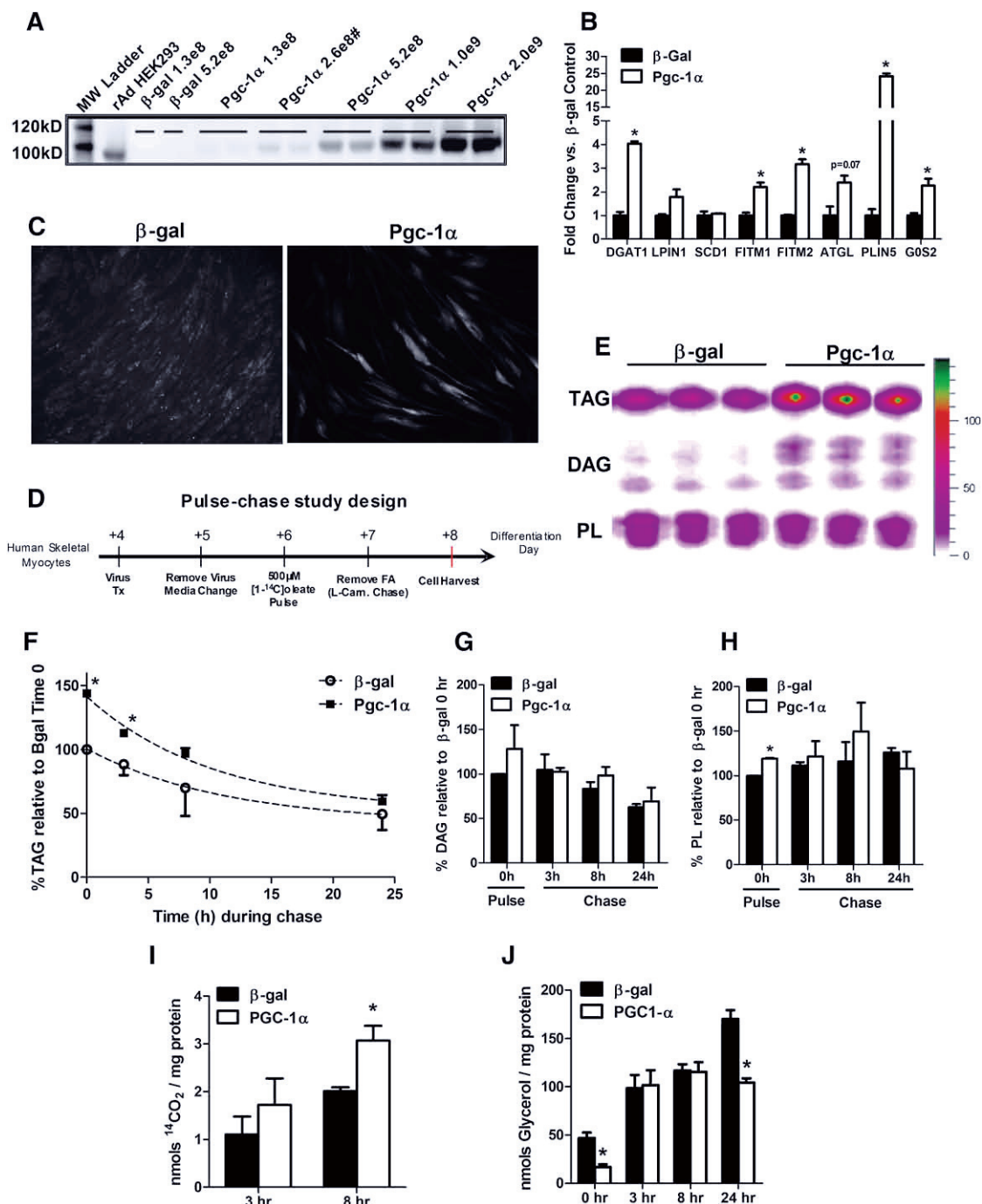


**Fig. 4.** Overexpression Pgc-1α affects lipid droplet metabolism in primary human skeletal muscle myotubes. (A) Western blot analysis of mouse Pgc-1α protein abundance in differentiation day 7 human skeletal myotubes. Cells were harvested 72 h after transduction with increasing doses (PFU/cm<sup>2</sup>) of adenoviruses expressing β-galactosidase (β-gal) or mouse Pgc-1α. (#) denotes the dose used for subsequent gene expression and pulse-chase studies. (B) mRNA expression analysis of myotubes harvested 72 h after virus treatment. Data are means ± SEM for triplicate wells from two independent experiments analyzed in triplicate and normalized to 18 s. (C) Day 4 myotubes were exposed to media containing 100 μM oleate/palmitate (1:1) bound to BSA at a 5:1 ratio for 72 h. Neutral lipids were stained using AdipoRed and visualized by fluorescent microscopy. (D) Schematic representation of the pulse-chase experimental design. L-carnitine (0.5 mM) was present only during the chase. (E) Representative radiogram of myotube lipids measured at the end of the 24 h pulse showing incorporation of [1-<sup>14</sup>C]oleate into TAG, DAG, and phospholipids (PL). Quantitation of [1-<sup>14</sup>C]oleate-labeling of (F) TAG, (G) DAG, and (H) PL during the pulse-chase experiment. Cells were harvested in 0.1% SDS lysis buffer at times 0 (immediately after the 24 h pulse), 3, 8, and 24 h during the carnitine chase. (I) <sup>14</sup>CO<sub>2</sub> production and (J) glycerol release into the medium at 3 and 8 h during the carnitine chase. Data are means ± SE of two independent experiments performed in triplicate and expressed as a percentage relative to levels in cells treated with β-gal virus at time 0 (the end of the pulse period). In (F–J), data are normalized to total cellular protein per well. \**P* < 0.05 versus β-gal treated control cells at the same time point.

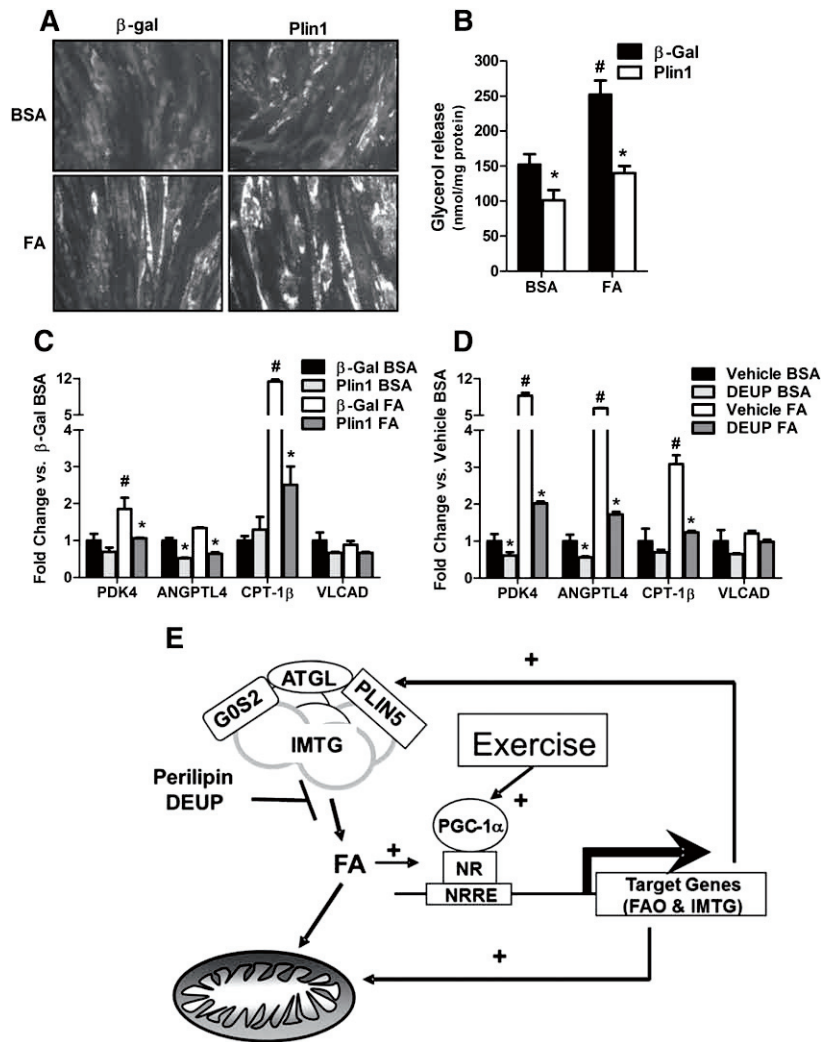


**Fig. 5.** Sequestering intramuscular triacylglycerol into lipid droplets blunts expression of PPAR target genes. Human skeletal myocytes were treated on differentiation day 4 with recombinant adenovirus ( $5.2 \times 10^8$  PFU/cm<sup>2</sup>) to express either  $\beta$ -galactosidase ( $\beta$ -gal) or mouse perilipin (Plp1). After 24 h, cells were treated an additional 72 h with 0.1% BSA or 0.1 mM oleate/palmitate (1:1) bound to BSA at a 5:1 ratio, followed by (A) neutral lipid staining with AdipoRed, (B) measurement of glycerol in the culture medium, and (C) gene expression analyses by RT-PCR. (D) On differentiation day 5, human myocytes were pretreated 24 h with 100  $\mu$ M of the lipase inhibitor diethylumbelliferyl phosphate (DEUP) or the vehicle alone (DMSO), followed by 72 h treatment with 0.1 mM oleate/palmitate (1:1) and measurement of gene expression. (E) Model showing the proposed metabolic interplay between lipid droplets and mitochondria. Data are means  $\pm$  SE of at least two independent experiments performed in triplicate. Glycerol was normalized to total cellular protein, and gene expression analyses were normalized to 18 s. \* $P < 0.05$  versus  $\beta$ -gal or vehicle control. # $P < 0.05$  versus BSA treatment.

To assess the translational relevance of the foregoing animal and cell-based studies, we next examined cross-sectional differences in expression of lipid droplet-associated proteins in muscle specimens biopsied from healthy young male subjects who were selected based on their levels of habitual physical activity. Detailed clinical and physiological characteristics of the study participants are provided in **Table 1**. As expected, increased fitness ( $\text{VO}_2$  max) in the trained compared with untrained subjects ( $61.5 \pm 3.7$  versus  $43.0 \pm 3.6$  ml/kg/min,  $P < 0.01$ ) was accompanied by elevated IMTG content, evident in both type I and type II myofibers (**Fig. 6A**), as well as a modest rise in muscle mRNA abundance of PGC-1 $\alpha$  ( $P = 0.059$ ) and several genes

involved in fatty acid uptake and catabolism (*PPAR $\alpha$* , *ERR $\alpha$* , *CD36*, *CPT1b*, and *MCAD*) (**Fig. 6B**). Similar to MCK-PGC-1 $\alpha$  transgenic mice, increased IMTG content in trained subjects corresponded with a 20–50% induction of transcripts encoding lipid droplet proteins, such as *ATGL*, *CGI58*, *PLIN2*, *PLIN5*, and *GOS2* (**Fig. 6B**). SCD1 mRNA levels also trended higher ( $\sim 2$ -fold;  $P = 0.07$ ) in trained subjects. Western blot analysis confirmed increased protein abundance of PLIN5 and PLIN2 in the trained compared with untrained state, whereas ATGL trended higher (**Fig. 6C**). CGI58 was not different between groups.

Lastly, we sought to explore potential relationships between muscle expression of lipid droplet genes and



TABLE 1. Clinical characteristics of the study population

Subject Characteristics	Untrained (n = 10)	Trained (n = 9)	P
	Mean $\pm$ SD	Mean $\pm$ SD	
Age (y)	21.9 $\pm$ 2.7	23.4 $\pm$ 2.7	NS
Weight (kg)	75.8 $\pm$ 9.5	67.8 $\pm$ 8.3	0.07
BMI (kg/m <sup>2</sup> )	22.8 $\pm$ 1.8	21.2 $\pm$ 1.7	0.05
Body fat (%)	19.1 $\pm$ 4.3	11.7 $\pm$ 3.4	<0.01
Fat mass (kg)	14.6 $\pm$ 4.5	8.0 $\pm$ 2.5	<0.01
Fat-free mass (kg)	61.1 $\pm$ 6.5	60.0 $\pm$ 7.6	NS
Change in glucose disposal rate ( $\Delta$ Rd)	35.7 $\pm$ 8.2	45.9 $\pm$ 8.6	<0.05
Fasting RQ	0.82 $\pm$ 0.02	0.80 $\pm$ 0.05	NS
Insulin-stimulated RQ <sup>a</sup>	0.91 $\pm$ 0.05	0.95 $\pm$ 0.01	<0.05
Metabolic flexibility ( $\Delta$ RQ)	0.09 $\pm$ 0.06	0.14 $\pm$ 0.05	<0.05
VO <sub>2</sub> max (ml/kg/min)	43.0 $\pm$ 3.6	61.5 $\pm$ 3.7	<0.01
Wmax (watt/kg)	3.7 $\pm$ 0.5	5.3 $\pm$ 0.6	<0.01
Fasting glucose (mmol/l)	5.0 $\pm$ 0.4	5.0 $\pm$ 0.2	NS
Fasting insulin (mU/ml)	10.7 $\pm$ 4.4	9.8 $\pm$ 3.3	NS
Basal EE (kcal/min)	1.90 $\pm$ 0.14	1.90 $\pm$ 0.09	NS
Basal GlcOx ( $\mu$ mol/kg/min)	9.7 $\pm$ 1.8	9.9 $\pm$ 4.6	NS
Basal LipidOx ( $\mu$ mol/kg/min)	1.21 $\pm$ 0.2	1.50 $\pm$ 0.4	0.08
Fasting FFA ( $\mu$ mol/l)	412.5 $\pm$ 146.5	282.8 $\pm$ 83.6	<0.05

All data are represented as mean  $\pm$  SD. GlcOx, glucose oxidation; LipidOx, lipid oxidation; NS, not significant.

<sup>a</sup> During a 6 h insulin infusion (40 mU/m<sup>2</sup> BSA/min) for a euglycemic-hyperinsulinemic clamp.

whole-body glucose homeostasis as assessed by a hyperinsulinemic-euglycemic clamp. In the basal condition, energy expenditure, substrate oxidation rates (glucose and lipid), and respiratory quotient (RQ) were similar between groups. Insulin sensitivity was elevated in the trained subjects,

evidenced by a 29% higher insulin-stimulated whole-body glucose disposal (Rd), which was principally attributable to oxidative glucose metabolism (Fig. 6D, E). Thus, the change in glucose oxidation in response to the clamp was 2-fold greater in trained than in untrained subjects

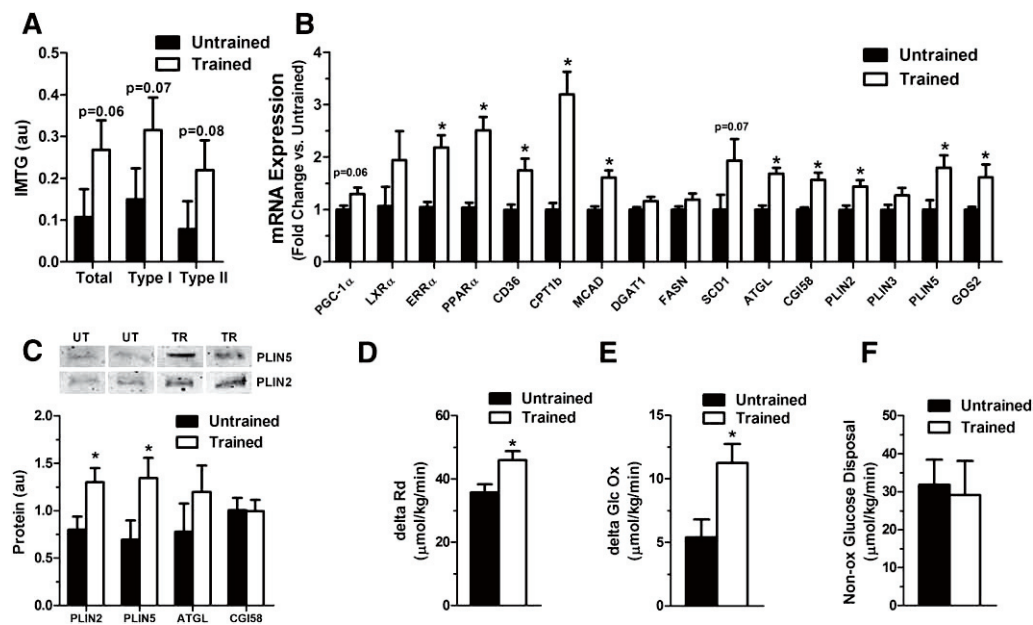


**Fig. 6.** Assessment of IMTG metabolism, fuel selection, and insulin action in trained compared with untrained human subjects. (A) Intramyocellular lipid content was measured by Oil Red O staining and combined with an immunofluorescence staining against slow myosin heavy chain (sMHC) to determine Type I fibers. Cells not stained for sMHC were considered to be Type II fibers. (B) mRNA levels of genes involved in lipid metabolism were measured by qRT-PCR in skeletal muscle tissue of trained compared with untrained men and expressed relative to GAPDH. (C) Representative blots and protein expression levels of lipid droplet coating (PLIN2, PLIN5) and lipolytic (ATGL, CGI58) proteins in skeletal muscles of trained compared with untrained men were measured by Western blot analysis. Insulin sensitivity expressed as insulin-stimulated change in (D) Rd ( $\Delta$ Rd), (E) glucose oxidation, and (F) nonoxidative glucose disposal during a euglycemic-hyperinsulinemic clamp with simultaneous infusion of glycerol. All parameters are expressed as  $\mu$ mol kg<sup>-1</sup> min<sup>-1</sup>. Untrained subjects (n = 9) are represented by black bars and trained subjects (n = 10) by white bars. Data expressed as mean  $\pm$  SE, \**P* < 0.05.

( $11.2 \pm 1.5$  versus  $5.4 \pm 1.4$   $\mu\text{mol/kg/min}$ ,  $P < 0.05$ ), whereas nonoxidative glucose disposal was similar between groups ( $31.8 \pm 2.8$  versus  $29.1 \pm 2.7$   $\mu\text{mol/kg/min}$ ,  $P = 0.50$ ; Fig. 6F). Notably, the insulin-induced shift in whole-body substrate selection (from fat to glucose oxidation), commonly dubbed “metabolic flexibility,” was much more robust in the trained subjects than in their sedentary counterparts ( $\Delta\text{RQ}$ :  $0.14 \pm 0.05$  versus  $0.09 \pm 0.06$  AU;  $P < 0.05$ ; Table 1).

A combination of univariate and stepwise linear regression analyses was used to examine interactions between fitness level ( $\text{VO}_2$  max), the lipid droplet program, and insulin action assessed by whole-body glucose disposal ( $\Delta\text{Rd}$ ) or metabolic flexibility ( $\Delta\text{RQ}$ ) in trained compared with untrained subjects. Univariate factors that correlated significantly ( $P < 0.05$ ) with  $\Delta\text{Rd}$  ( $\text{VO}_2$  max, along with ATGL and PLIN5 mRNA and protein abundance) and  $\Delta\text{RQ}$  ( $\text{VO}_2$  max, ATGL protein and mRNA expression, and SCD1 mRNA expression) were added to a stepwise linear regression analysis run within each group (trained versus untrained). Because G0S2 regulates ATGL activity (23) and was robustly induced by exercise in both mice and humans, we also included G0S2 mRNA expression in these models. In trained subjects, dominant predictors of  $\Delta\text{Rd}$  included  $\text{VO}_2$  max, PLIN5 mRNA and protein expression, along with ATGL and G0S2 mRNA abundance (model  $R^2 = 0.99$ ,  $P < 0.05$ ; Table 2). Predictors of  $\Delta\text{RQ}$  included ATGL, SCD1, and G0S2 mRNA expression (model  $R^2 = 0.89$ ,  $P < 0.05$ ; Table 2). In the untrained subjects, only G0S2 mRNA levels predicted  $\Delta\text{Rd}$  (model  $R^2 = 0.61$ ,  $P < 0.05$ ; Table 2) and  $\Delta\text{RQ}$  (model  $R^2 = 0.49$ ,  $P < 0.05$ ; Table 2). In aggregate, these results build on evidence that exercise-induced adaptations in IMTG metabolism contribute positively to glucose homeostasis in trained subjects (34–37).

## DISCUSSION

PGC-1 $\alpha$  is a promiscuous transcriptional coactivator that plays a prominent role in regulating mitochondrial genesis, oxidative metabolism, and muscle adaption to exercise (10, 24, 38, 39). More recently, investigators suggested that PGC-1 $\alpha$  might also promote intramuscular lipid storage (40, 41). For example, gastrocnemius muscles from MCK-PGC-1 $\alpha$  transgenic mice were found to have elevated TAG and DAG after high-fat feeding (39), whereas a subsequent report concluded that intramuscular lipid accumulation in these mice is secondary to specific

activation of the de novo lipogenesis pathway (41). Herein, we provide novel evidence that PGC-1 $\alpha$  targets a number of genes involved in lipid droplet assembly and mobilization. Accordingly, heightened activity of PGC-1 $\alpha$  in mouse TA muscles resulted in increased IMTG and DAG content, even when animals were fed a standard (low-fat) chow diet. Importantly, we also identified a positive association between exercise training, PGC-1 $\alpha$  abundance, and expression of lipid droplet genes in human skeletal muscle. When results of the animal, cell-based, and human studies are taken together, transcriptional regulation of the lipid droplet program was clearly manifest as functional changes in lipid droplet synthesis, turnover, and enhanced oxidation of TAG-derived fatty acids. Also noteworthy is that our experiments revealed a subset of lipid droplet-related genes that were upregulated by acute exercise but unchanged in muscles from the MCK-PGC1a transgenic mice. Thus, it appears that regulatory signals other than PGC-1 $\alpha$  activation are required for the full effect of exercise on the lipid droplet program.

Lipid droplets have gained increasing recognition as bona fide organelles that participate in a diverse array of cellular functions. These particles are decorated and regulated by a complex and dynamic network of lipid droplet coat proteins that orchestrate droplet assembly, size, localization, and mobilization (42). Some of these proteins are permanent residents, whereas others appear to associate with the droplets in a transient manner, depending on the physiological setting. The best-studied members of this class of proteins belong to the PAT/perilipin family, which includes Plin 1, ADRP/Plin2, TIP47/Plin3, Plin 4, and Plin5 (43). In the present study, Plin5 clearly stood out as the most responsive lipid droplet target gene of PGC-1 $\alpha$ . Here and in another recent study (44), PLIN5 protein expression was found to be elevated in muscles of exercise-trained humans. The precise function of this protein remains unclear, but several lines of evidence point to a key role for Plin5 in governing the spatial and metabolic interactions between lipid intramuscular droplets and their surrounding mitochondrial reticulum (45–48).

The recent spotlight on lipid droplets has led investigators to question whether and how lipid molecules generated during lipolysis are directed toward specific metabolic fates and/or signaling pathways. For example, emerging evidence suggests that lipid droplets per se provide an important and perhaps essential source of ligands for the PPAR family of transcription factors (28–30). Consistent with this paradigm, we found that disrupting IMTG mobilization via genetic or pharmacological maneuvers dampened

TABLE 2. Significant correlates of insulin sensitivity and metabolic flexibility in trained and untrained subjects


Clinical Characteristic	Input Variables	Significant Correlates	R <sup>2</sup>	P
Trained				
Insulin sensitivity ( $\Delta\text{Rd}$ )	$\text{VO}_2$ max, PLIN5, ATGL, G0S2	$\text{VO}_2$ max, PLIN5, ATGL, G0S2	0.99	<0.05
Metabolic flexibility ( $\Delta\text{RQ}$ )	$\text{VO}_2$ max, SCD1, ATGL, G0S2	ATGL, SCD1, G0S2	0.89	<0.05
Untrained				
Insulin sensitivity ( $\Delta\text{Rd}$ )	$\text{VO}_2$ max, PLIN5, ATGL, G0S2	G0S2	0.61	<0.05
Metabolic flexibility ( $\Delta\text{RQ}$ )	$\text{VO}_2$ max, SCD1, ATGL, G0S2	G0S2	0.49	<0.05

All data are presented as R<sup>2</sup>.

expression of several PPAR target genes in primary HS-kMC. These findings support a model in which PGC-1 $\alpha$ -mediated enhancement of IMTG synthesis and turnover serves as a feed-forward mechanism to maintain the mitochondrial machinery that facilitates lipid catabolism (Fig. 5E). On a more conspicuous level, IMTG also serve as a potential source of oxidative substrate. Numerous studies have confirmed the use of IMTG during various modes of exercise (reviewed in Refs. 49, 50). Interestingly, the best-trained athletes tend to have the highest IMTG content prior to exercise and the greatest depletion at the end of the event (51, 52), implying that training actually enhances muscle reliance on local lipids. By contrast, the extent to which mobilization and oxidation of IMTG occurs during rest is less clear and more controversial. Herein, we used isolated mouse soleus and EDL to show that both muscle types draw on endogenous lipid reserves under quiescent conditions, implying that IMTG also play a role in supporting resting energy expenditure.

Whereas our findings provide new insights into the molecular basis for IMTG accumulation in trained muscles, the question of why these lipids do not impinge upon glucose homeostasis in physically active individuals remains unanswered. Although the explanation for this “athlete’s paradox” is probably complex at a molecular level, it is tempting to speculate that the lipid droplet proteome resident within trained muscles might permit tighter control over intracellular lipid trafficking. For example, upregulation of triacylglycerol biosynthetic enzymes might facilitate rapid esterification and/or reesterification of fatty acids that are not needed as oxidative substrates. Conversely, the enhanced lipolytic potential conferred by elevated ATGL expression is likely to boost rates of IMTG mobilization when demand for fatty acid fuel rises. ATGL is a ubiquitously expressed lipase that selectively performs the first step in TAG hydrolysis. Its catalytic activity increases dramatically in the presence of CGI-58, a coactivator that binds to both ATGL and the lipid droplet surface via distinct domains (53). ATGL also binds PLIN5 and G0S2, both of which modulate lipolysis by altering the interaction between ATGL and CGI-58. For instance, ectopic expression PLIN5 in CHO cells protected against ATGL-mediated lipolysis in the basal state but enhanced lipolytic activity under adrenergically stimulated conditions (54). Another recent report showed that G0S2 acts as a potent insulin-inducible inhibitor of ATGL hydrolase activity, even in the presence of CGI-58 (55). Thus, the cadre of lipid droplet genes that are induced by exercise and PGC-1 $\alpha$  exerts control over glycerolipid hydrolysis in both directions, possibly conferring enhanced regulatory capacity to rapidly modulate lipid mobilization according to metabolic demand.

In the context of this discussion, it is noteworthy that muscle fuel selection is disrupted in obese and insulin-resistant states (36, 56–58). Under healthy conditions, this tissue harbors robust capacity to adjust substrate preference in response to nutrient and hormonal cues. This versatility is classically evident during the transition between fasting and feeding (herein mimicked by the clamp condition),

when heavy reliance on fatty acid subsides to permit use of the newly available glucose. By contrast, in obese rodents and humans, this switch in metabolic currency fails, thereby reflecting a state of “metabolic inflexibility” (36, 56–58). The molecular basis of this phenomenon remains murky, but poorly controlled mobilization and reesterification of IMTG-derived fatty acids could conceivably play a role. Accordingly, we speculate that the lipid droplets assembled in response to exercise training allow the muscles to better manage a heavy influx of fatty acid fuel and that precisely regulated trafficking of substrate to and from IMTG contributes to optimal mitochondrial performance and metabolic flexibility. This interpretation is consistent with our observation that insulin-stimulated substrate switching from fatty acid to glucose oxidation was markedly enhanced in trained subjects, despite elevated IMTG content. Moreover, stepwise regression analyses identified ATGL, PLIN5, and G0S2 as strong predictors of insulin sensitivity and metabolic flexibility, particularly in the trained subjects, suggesting that appropriate activation and termination of intramuscular lipolysis bears heavily on these traits. Although these correlative results are not definitive, they do point toward a new and provocative avenue for future investigations. 

The authors thank Dr. Andy Greenberg at Tufts University for providing the Plin1 adenovirus and Dr. Bruce Spiegelman at Harvard University for providing the MCK-PGC1 $\alpha$  transgenic mice for these studies. The authors kindly recognize Victoria Madden and Steven Ray from the Microscopy Services Laboratory, Dept. of Pathology and Laboratory Medicine, UNC-Chapel Hill, for their technical expertise with transmission electron microscopy.

## REFERENCES

1. Muoio, D. M., and C. B. Newgard. 2008. Mechanisms of disease: molecular and metabolic mechanisms of insulin resistance and beta-cell failure in type 2 diabetes. *Nat. Rev. Mol. Cell Biol.* **9**: 193–205.
2. Bosma, M., S. Kersten, M. K. Hesselink, and P. Schrauwen. 2012. Re-evaluating lipotoxic triggers in skeletal muscle: relating intramyocellular lipid metabolism to insulin sensitivity. *Prog. Lipid Res.* **51**: 36–49.
3. Goodpaster, B. H., J. He, S. Watkins, and D. E. Kelley. 2001. Skeletal muscle lipid content and insulin resistance: evidence for a paradox in endurance-trained athletes. *J. Clin. Endocrinol. Metab.* **86**: 5755–5761.
4. Krssak, M., K. Falk Petersen, A. Dresner, L. DiPietro, S. M. Vogel, D. L. Rothman, M. Roden, and G. I. Shulman. 1999. Intramyocellular lipid concentrations are correlated with insulin sensitivity in humans: a 1H NMR spectroscopy study. *Diabetologia.* **42**: 113–116.
5. Perseghin, G., P. Scifo, F. De Cobelli, E. Pagliato, A. Battezzati, C. Arcelloni, A. Vanzulli, G. Testolin, G. Pozza, A. Del Maschio, et al. 1999. Intramyocellular triglyceride content is a determinant of in vivo insulin resistance in humans: a 1H–13C nuclear magnetic resonance spectroscopy assessment in offspring of type 2 diabetic parents. *Diabetes.* **48**: 1600–1606.
6. Dube, J. J., F. Amati, M. Stefanovic-Racic, F. G. Toledo, S. E. Sauers, and B. H. Goodpaster. 2008. Exercise-induced alterations in intramyocellular lipids and insulin resistance: the athlete’s paradox revisited. *Am. J. Physiol. Endocrinol. Metab.* **294**: E882–E888.
7. Shaw, C. S., D. A. Jones, and A. J. Wagenmakers. 2008. Network distribution of mitochondria and lipid droplets in human muscle fibres. *Histochem. Cell Biol.* **129**: 65–72.
8. Reynolds, E. S. 1963. The use of lead citrate at high pH as an electron-opaque stain in electron microscopy. *J. Cell Biol.* **17**: 208–212.



9. Muoio, D. M., K. Seefeld, L. A. Witters, and R. A. Coleman. 1999. AMP-activated kinase reciprocally regulates triacylglycerol synthesis and fatty acid oxidation in liver and muscle: evidence that sn-glycerol-3-phosphate acyltransferase is a novel target. *Biochem. J.* **338**: 783–791.
10. Koves, T. R., P. Li, J. An, T. Akimoto, D. Slentz, O. Ilkayeva, G. L. Dohm, Z. Yan, C. B. Newgard, and D. M. Muoio. 2005. Peroxisome proliferator-activated receptor-gamma co-activator 1alpha-mediated metabolic remodeling of skeletal myocytes mimics exercise training and reverses lipid-induced mitochondrial inefficiency. *J. Biol. Chem.* **280**: 33588–33598.
11. Muoio, D. M., J. M. Way, C. J. Tanner, D. A. Winegar, S. A. Klierer, J. A. Houmard, W. E. Kraus, and G. L. Dohm. 2002. Peroxisome proliferator-activated receptor-alpha regulates fatty acid utilization in primary human skeletal muscle cells. *Diabetes*. **51**: 901–909.
12. Kien, C. L., K. I. Everingham, R. D. Stevens, N. K. Fukagawa, and D. M. Muoio. 2011. Short-term effects of dietary fatty acids on muscle lipid composition and serum acylcarnitine profile in human subjects. *Obesity (Silver Spring)*. **19**: 305–311.
13. Becker, T. C., R. J. Noel, W. S. Coats, A. M. Gomez-Foix, T. Alam, R. D. Gerard, and C. B. Newgard. 1994. Use of recombinant adenovirus for metabolic engineering of mammalian cells. *Methods Cell Biol.* **43(Pt A)**: 161–189.
14. Koopman, R., G. Schaart, and M. K. Hesselink. 2001. Optimisation of Oil Red O staining permits combination with immunofluorescence and automated quantification of lipids. *Histochem. Cell Biol.* **116**: 63–68.
15. Chomczynski, P., and N. Sacchi. 1987. Single-step method of RNA isolation by acid guanidinium thiocyanate-phenol-chloroform extraction. *Anal. Biochem.* **162**: 156–159.
16. Bustin, S. A. 2000. Absolute quantification of mRNA using real-time reverse transcription polymerase chain reaction assays. *J. Mol. Endocrinol.* **25**: 169–193.
17. Thyfault, J. P., M. G. Cree, D. Zheng, J. J. Zwetsloot, E. B. Tapscott, T. R. Koves, O. Ilkayeva, R. R. Wolfe, D. M. Muoio, and G. L. Dohm. 2007. Contraction of insulin-resistant muscle normalizes insulin action in association with increased mitochondrial activity and fatty acid catabolism. *Am. J. Physiol. Cell Physiol.* **292**: C729–C739.
18. Schoiswohl, G., M. Schweiger, R. Schreiber, G. Gorkiewicz, K. Preiss-Landl, U. Taschler, K. A. Zierler, F. P. Radner, T. O. Eichmann, P. C. Kienesberger, et al. 2010. Adipose triglyceride lipase plays a key role in the supply of the working muscle with fatty acids. *J. Lipid Res.* **51**: 490–499.
19. Russell, A. P., M. K. Hesselink, S. K. Lo, and P. Schrauwen. 2005. Regulation of metabolic transcriptional co-activators and transcription factors with acute exercise. *FASEB J.* **19**: 986–988.
20. Baar, K., A. R. Wende, T. E. Jones, M. Marison, L. A. Nolte, M. Chen, D. P. Kelly, and J. O. Holloszy. 2002. Adaptations of skeletal muscle to exercise: rapid increase in the transcriptional coactivator PGC-1. *FASEB J.* **16**: 1879–1886.
21. Pilegaard, H., B. Saltin, and P. D. Neuffer. 2003. Exercise induces transient transcriptional activation of the PGC-1alpha gene in human skeletal muscle. *J. Physiol.* **546**: 851–858.
22. Akimoto, T., S. C. Pohnert, P. Li, M. Zhang, C. Gumbs, P. B. Rosenberg, R. S. Williams, and Z. Yan. 2005. Exercise stimulates Pgc-1alpha transcription in skeletal muscle through activation of the p38 MAPK pathway. *J. Biol. Chem.* **280**: 19587–19593.
23. Kadereit, B., P. Kumar, W. J. Wang, D. Miranda, E. L. Snapp, N. Severina, I. Torregroza, T. Evans, and D. L. Silver. 2008. Evolutionarily conserved gene family important for fat storage. *Proc. Natl. Acad. Sci. USA*. **105**: 94–99.
24. Lin, J., H. Wu, P. T. Tarr, C. Y. Zhang, Z. Wu, O. Boss, L. F. Michael, P. Puigserver, E. Isotani, E. N. Olson, et al. 2002. Transcriptional co-activator PGC-1 alpha drives the formation of slow-twitch muscle fibres. *Nature*. **418**: 797–801.
25. Wolins, N. E., B. K. Quaynor, J. R. Skinner, A. Tzekov, M. A. Croce, M. C. Gropler, V. Varma, A. Yao-Borengasser, N. Rasouli, P. A. Kern, et al. 2006. OXPAT/PAT-1 is a PPAR-induced lipid droplet protein that promotes fatty acid utilization. *Diabetes*. **55**: 3418–3428.
26. Schultz, C. J., E. Torres, C. Londos, and J. S. Torday. 2002. Role of adipocyte differentiation-related protein in surfactant phospholipid synthesis by type II cells. *Am. J. Physiol. Lung Cell. Mol. Physiol.* **283**: L288–L296.
27. Russell, A. P., J. Feilchenfeldt, S. Schreiber, M. Praz, A. Crettenand, C. Gobelet, C. A. Meier, D. R. Bell, A. R. Giacobino, et al. 2003. Endurance training in humans leads to fiber type-specific increases in levels of peroxisome proliferator-activated receptor-gamma coactivator-1 and peroxisome proliferator-activated receptor-alpha in skeletal muscle. *Diabetes*. **52**: 2874–2881.
28. Ahmadian, M., M. J. Abbott, T. Tang, C. S. Hudak, Y. Kim, M. Bruss, M. K. Hellerstein, H. Y. Lee, V. T. Samuel, G. I. Shulman, et al. 2011. Desnutrin/ATGL is regulated by AMPK and is required for a brown adipose phenotype. *Cell Metab.* **13**: 739–748.
29. Ong, K. T., M. T. Mashek, S. Y. Bu, A. S. Greenberg, and D. G. Mashek. 2011. Adipose triglyceride lipase is a major hepatic lipase that regulates triacylglycerol turnover and fatty acid signaling and partitioning. *Hepatology*. **53**: 116–126.
30. Haemmerle, G., T. Moustafa, G. Woelkart, S. Buttner, A. Schmidt, T. van de Weijer, M. Hesselink, D. Jaeger, P. C. Kienesberger, K. Zierler, et al. 2011. ATGL-mediated fat catabolism regulates cardiac mitochondrial function via PPAR-alpha and PGC-1. *Nat. Med.* **17**: 1076–1085.
31. Greenberg, A. S., J. J. Egan, S. A. Wek, N. B. Garty, E. J. Blanchette-Mackie, and C. Londos. 1991. Perilipin, a major hormonally regulated adipocyte-specific phosphoprotein associated with the periphery of lipid storage droplets. *J. Biol. Chem.* **266**: 11341–11346.
32. Egan, J. J., A. S. Greenberg, M. K. Chang, and C. Londos. 1990. Control of endogenous phosphorylation of the major cAMP-dependent protein kinase substrate in adipocytes by insulin and beta-adrenergic stimulation. *J. Biol. Chem.* **265**: 18769–18775.
33. Singh, R., S. Kaushik, Y. Wang, Y. Xiang, I. Novak, M. Komatsu, K. Tanaka, A. M. Cuervo, and M. J. Czaja. 2009. Autophagy regulates lipid metabolism. *Nature*. **458**: 1131–1135.
34. Liu, L., Y. Zhang, N. Chen, X. Shi, B. Tsang, and Y. H. Yu. 2007. Upregulation of myocellular DGAT1 augments triglyceride synthesis in skeletal muscle and protects against fat-induced insulin resistance. *J. Clin. Invest.* **117**: 1679–1689.
35. Schenk, S., and J. F. Horowitz. 2007. Acute exercise increases triglyceride synthesis in skeletal muscle and prevents fatty acid-induced insulin resistance. *J. Clin. Invest.* **117**: 1690–1698.
36. Meex, R. C., V. B. Schrauwen-Hinderling, E. Moonen-Kornips, G. Schaart, M. Mensink, E. Phielix, T. van de Weijer, J. P. Sels, P. Schrauwen, and M. K. Hesselink. 2010. Restoration of muscle mitochondrial function and metabolic flexibility in type 2 diabetes by exercise training is paralleled by increased myocellular fat storage and improved insulin sensitivity. *Diabetes*. **59**: 572–579.
37. Phillips, S. A., C. C. Choe, T. P. Ciaraldi, A. S. Greenberg, A. P. Kong, S. C. Baxi, L. Christiansen, S. R. Mudaliar, and R. R. Henry. 2005. Adipocyte differentiation-related protein in human skeletal muscle: relationship to insulin sensitivity. *Obes. Res.* **13**: 1321–1329.
38. Summermatter, S., H. Troxler, G. Santos, and C. Handschin. 2011. Coordinated balancing of muscle oxidative metabolism through PGC-1alpha increases metabolic flexibility and preserves insulin sensitivity. *Biochem. Biophys. Res. Commun.* **408**: 180–185.
39. Choi, C. S., D. E. Befroy, R. Codella, S. Kim, R. M. Reznick, Y. J. Hwang, Z. X. Liu, H. Y. Lee, A. Distefano, V. T. Samuel, et al. 2008. Paradoxical effects of increased expression of PGC-1alpha on muscle mitochondrial function and insulin-stimulated muscle glucose metabolism. *Proc. Natl. Acad. Sci. USA*. **105**: 19926–19931.
40. Espinoza, D. O., L. G. Boros, S. Crunkhorn, H. Gami, and M. E. Patti. 2010. Dual modulation of both lipid oxidation and synthesis by peroxisome proliferator-activated receptor-gamma coactivator-1alpha and -1beta in cultured myotubes. *FASEB J.* **24**: 1003–1014.
41. Summermatter, S., O. Baum, G. Santos, H. Hoppeler, and C. Handschin. 2010. Peroxisome proliferator-activated receptor [gamma] coactivator 1[alpha] (PGC-1[alpha]) promotes skeletal muscle lipid refueling in vivo by activating de novo lipogenesis and the pentose phosphate pathway. *J. Biol. Chem.* **285**: 32793–32800.
42. Lass, A., R. Zimmermann, M. Oberer, and R. Zechner. 2011. Lipolysis - a highly regulated multi-enzyme complex mediates the catabolism of cellular fat stores. *Prog. Lipid Res.* **50**: 14–27.
43. Bickel, P. E., J. T. Tansey, and M. A. Welte. 2009. PAT proteins, an ancient family of lipid droplet proteins that regulate cellular lipid stores. *Biochim. Biophys. Acta*. **1791**: 419–440.
44. Amati, F., J. J. Dube, E. Alvarez-Carnero, M. M. Edreira, P. Chomentowski, P. M. Coen, G. E. Switzer, P. E. Bickel, M. Stefanovic-Racic, F. G. Toledo, et al. 2011. Skeletal muscle triglycerides, diacylglycerols, and ceramides in insulin resistance: another paradox in endurance-trained athletes? *Diabetes*. **60**: 2588–2597.
45. Bosma, M., M. K. Hesselink, L. M. Sparks, S. Timmers, M. J. Ferraz, F. Mattijssen, D. van Beurden, G. Schaart, M. H. de Baets, F. K. Verheyen, et al. 2012. Perilipin 2 improves insulin sensitivity in skeletal muscle despite elevated intramuscular lipid levels. *Diabetes*. **61**: 2679–2690.

46. Wang, H., U. Sreenivasan, H. Hu, A. Saladino, B. M. Polster, L. M. Lund, D. W. Gong, W. C. Stanley, and C. Sztalryd. 2011. Perilipin 5, a lipid droplet-associated protein, provides physical and metabolic linkage to mitochondria. *J. Lipid Res.* **52**: 2159–2168.
47. Pidoux, G., O. Witczak, E. Jarnaess, L. Myrvold, H. Urlaub, A. J. Stokka, T. Kuntziger, and K. Tasken. 2011. Optic atrophy 1 is an A-kinase anchoring protein on lipid droplets that mediates adrenergic control of lipolysis. *EMBO J.* **30**: 4371–4386.
48. Bosma, M., R. Minnaard, L. M. Sparks, G. Schaart, M. Losen, M. H. de Baets, H. Duimel, S. Kersten, P. E. Bickel, P. Schrauwen, et al. 2012. The lipid droplet coat protein perilipin 5 also localizes to muscle mitochondria. *Histochem. Cell Biol.* **137**: 205–216.
49. Schrauwen-Hinderling, V. B., M. K. Hesselink, P. Schrauwen, and M. E. Kooi. 2006. Intramyocellular lipid content in human skeletal muscle. *Obesity (Silver Spring)*. **14**: 357–367.
50. Shaw, C. S., J. Clark, and A. J. Wagenmakers. 2010. The effect of exercise and nutrition on intramuscular fat metabolism and insulin sensitivity. *Annu. Rev. Nutr.* **30**: 13–34.
51. Lithell, H., J. Orlander, R. Schele, B. Sjodin, and J. Karlsson. 1979. Changes in lipoprotein-lipase activity and lipid stores in human skeletal muscle with prolonged heavy exercise. *Acta Physiol. Scand.* **107**: 257–261.
52. Hurley, B. F., P. M. Nemeth, W. H. Martin 3rd, J. M. Hagberg, G. P. Dalsky, and J. O. Holloszy. 1986. Muscle triglyceride utilization during exercise: effect of training. *J. Appl. Physiol.* **60**: 562–567.
53. Lu, X., X. Yang, and J. Liu. 2010. Differential control of ATGL-mediated lipid droplet degradation by CGI-58 and G0S2. *Cell Cycle*. **9**: 2719–2725.
54. Wang, H., M. Bell, U. Sreenivasan, H. Hu, J. Liu, K. Dalen, C. Londos, T. Yamaguchi, M. A. Rizzo, R. Coleman, et al. 2011. Unique regulation of adipose triglyceride lipase (ATGL) by perilipin 5, a lipid droplet-associated protein. *J. Biol. Chem.* **286**: 15707–15715.
55. Yang, X., X. Lu, M. Lombes, G. B. Rha, Y. I. Chi, T. M. Guerin, E. J. Smart, and J. Liu. 2010. The G(0)/G(1) switch gene 2 regulates adipose lipolysis through association with adipose triglyceride lipase. *Cell Metab.* **11**: 194–205.
56. Kelley, D. E., B. Goodpaster, R. R. Wing, and J. A. Simoneau. 1999. Skeletal muscle fatty acid metabolism in association with insulin resistance, obesity, and weight loss. *Am. J. Physiol.* **277**: E1130–E1141.
57. Koves, T. R., J. R. Ussher, R. C. Noland, D. Slentz, M. Mosedale, O. Ilkayeva, J. Bain, R. Stevens, J. R. Dyck, C. B. Newgard, et al. 2008. Mitochondrial overload and incomplete fatty acid oxidation contribute to skeletal muscle insulin resistance. *Cell Metab.* **7**: 45–56.
58. Noland, R. C., T. R. Koves, S. E. Seiler, H. Lum, R. M. Lust, O. Ilkayeva, R. D. Stevens, F. G. Hegardt, and D. M. Muoio. 2009. Carnitine insufficiency caused by aging and overnutrition compromises mitochondrial performance and metabolic control. *J. Biol. Chem.* **284**: 22840–22852.